Effect of frequency and power on the piezocatalytic and sonochemical degradation of dyes in water

Bößl, F., Menzel, V. C., Chatzisymeon, E., Comyn, T. P., Cowin, P., Cobley, A. J. & Tudela, I

DOI 10.1016/j.ceja.2023.100477
ISSN 2666-8211

Publisher: Elsevier

Chemical Engineering Journal Advances 14 (2023) 100477

Contents lists available at ScienceDirect

Chemical Engineering Journal Advances

journal homepage: www.sciencedirect.com/journal/chemical-engineering-journal-advances

Effect of frequency and power on the piezocatalytic and sonochemical degradation of dyes in water

Franziska Bößl [a,*], Valentin C. Menzel [a], Efthalia Chatzisymeon [b], Tim P. Comyn [c], Peter Cowin [c], Andrew J. Cobley [d], Ignacio Tudela [a,*]

[a] School of Engineering, Institute for Materials and Processes, Edinburgh Electrochemical Engineering Group (e3 Group), The University of Edinburgh, Sanderson Building, Robert Stevenson Road, Edinburgh, EH9 3FB, United Kingdom
[b] School of Engineering, Institute for Infrastructure and Environment, The University of Edinburgh, William Rankine Building, Thomas Bayes Road, Edinburgh, EH9 3JL, United Kingdom
[c] Ionix Advanced Technologies Ltd., 3M Buckley Innovation Centre, Firth Street, Huddersfield, HD1 3BD, United Kingdom
[d] Functional Materials and Chemistry Research Group, Research Centre for Manufacturing and Materials, Institute of Clean Growth and Future Mobility, Coventry University, Beresford Avenue, Coventry, CV6 5LZ, United Kingdom

ARTICLE INFO

Keywords:
Piezocatalysis
Sonochemistry
Dye degradation
Cavitation
Ultrasonic frequency
Ultrasonic power

ABSTRACT

For the very first time, the effect of frequency on the piezocatalytic degradation of dyes has been systematically evaluated. To achieve this, a combination of systems and experimental setups operating at different ultrasonic frequencies ranging from 20 kHz up to 1 MHz were used. In addition, the effect of ultrasonic power was investigated at a low ultrasonic frequency of 20 kHz and higher ultrasonic frequency of 576 kHz to shed more light into the controversial discussion surrounding the 'true' mechanisms behind piezocatalysis. The results revealed that mechanical effects derived from acoustic cavitation, predominant at lower ultrasonic frequencies (<100 kHz), indeed enhanced the piezocatalytic degradation of the dye, Rhodamine B, to some extent (from 53% to 64% RhB degradation after 2 h). However, it was again demonstrated that sonochemical production of radicals remains a significant contributor for the overall degradation of the dye. Moreover, at higher ultrasonic frequencies (>100 kHz), the chemical effects derived from acoustic cavitation were so remarkable, that it raised the question of whether a piezocatalyst is really necessary when the optimisation of frequency and power may be enough for sonochemistry to fully degrade organic pollutants at a fast rate (pseudo first-order degradation reaction rate constant up to 0.037 min^{-1}).

1. Introduction

Piezocatalysis is a new concept in the field of catalysis that has attracted much attention in recent years. This novel area of research is considered a promising development within catalysis due to the potential use of renewable and prevalent vibrations such as those from wind or tides that could make catalytic reactions independent from energy sources like electricity and light [1–8]. Piezocatalysis aims to take advantage of piezoelectric materials that have the ability to generate an electrical response while being strained or stressed by an external force. This external force is commonly applied by a mechanical field (i.e. acoustic field generated by ultrasound) [5-7,9-16] surrounding the piezoelectric materials, leading to redox reactions occurring over the surface of such materials (i.e. piezocatalyst).

Despite numerous reports on piezocatalytic processes [4,7,11-15, 17-22], the mechanism of piezocatalysis remains controversial [1,23]. In recent years, two very different potential mechanisms have been suggested for piezocatalysis [1-4,21-24]. On the one hand, researchers have considered energy band theory analogous to photocatalysis, where redox reactions occurring at the surface of piezocatalysts are determined by the energy band levels from the valence and conduction bands. On the other hand, researchers have referred to more classical piezoelectricity (either bulk or localised piezoelectric polarisation) where the piezoelectric potential is the driving force of chemical reactions at the piezocatalyst surface.

If bulk piezoelectric polarisation resulting from the piezoelectric potential was the dominant mechanism behind piezocatalysis (Fig. 1a), achieving the maximum piezoelectric polarisation within a

* Corresponding author.
E-mail addresses: f.boessl@ed.ac.uk (F. Bößl), ignacio.tudela@ed.ac.uk (I. Tudela).

https://doi.org/10.1016/j.ceja.2023.100477

Available online 4 March 2023

piezocatalyst would obviously result in an enhanced performance of the process. In general, a piezoelectric material will exhibit a higher piezoelectric response when excited at its resonance frequency, or at a global resonance frequency of the whole mechanical system [25,26] where said piezoelectric material is being used (a piezocatalyst particle and a surrounding liquid in the present case). Hence, one would expect a higher piezocatalytic effect if a piezocatalyst was excited close to either its resonance frequency or a global resonance frequency of the system that could result in a high piezoelectric polarisation. However, the vast majority of research on piezocatalysis has only used low-power acoustic vibrations around 40 kHz [5-7,9-16,27,28] as the main method to mechanically excite piezocatalysts, far from their resonance frequencies (which should be in the MHz order of magnitude) and without consideration for global resonance frequencies of the whole mechanical system involved. Only recently the research community has started to explore the possibility of conducting piezocatalytical processes at different frequencies, but with a focus on the low range (<100 kHz) [17]. If piezocatalysts were truly excited at frequencies close to their resonance frequencies or the global resonance frequency of the system (i.e. frequencies where a significantly higher degree of bulk piezoelectric polarisation could be achieved), one would expect a remarkable enhancement of the piezocatalytic behaviour. If this was not the case, though, it would confirm the unviability of that proposed mechanism, shedding more light onto how piezocatalysis really works.

As previously reported by the authors [29] and more recently confirmed by other researchers [6], other phenomena such as sonochemistry (Fig. 1c) or sonocatalysis are also likely to occur when studying piezocatalysis whenever ultrasound is used to generate an acoustic field as the method to excite piezocatalysts, as this will also result in the occurrence of acoustic cavitation driving such phenomena. These phenomena are also severely influenced by both frequency and power of ultrasounds [30–33]. Therefore, the aim of this study is to evaluate and understand, from both piezocatalytic and sonochemical point of view, the effect that ultrasonic frequency and power have on the overall piezocatalytic process to find out whether bulk piezoelectric polarisation is really behind piezocatalysis.

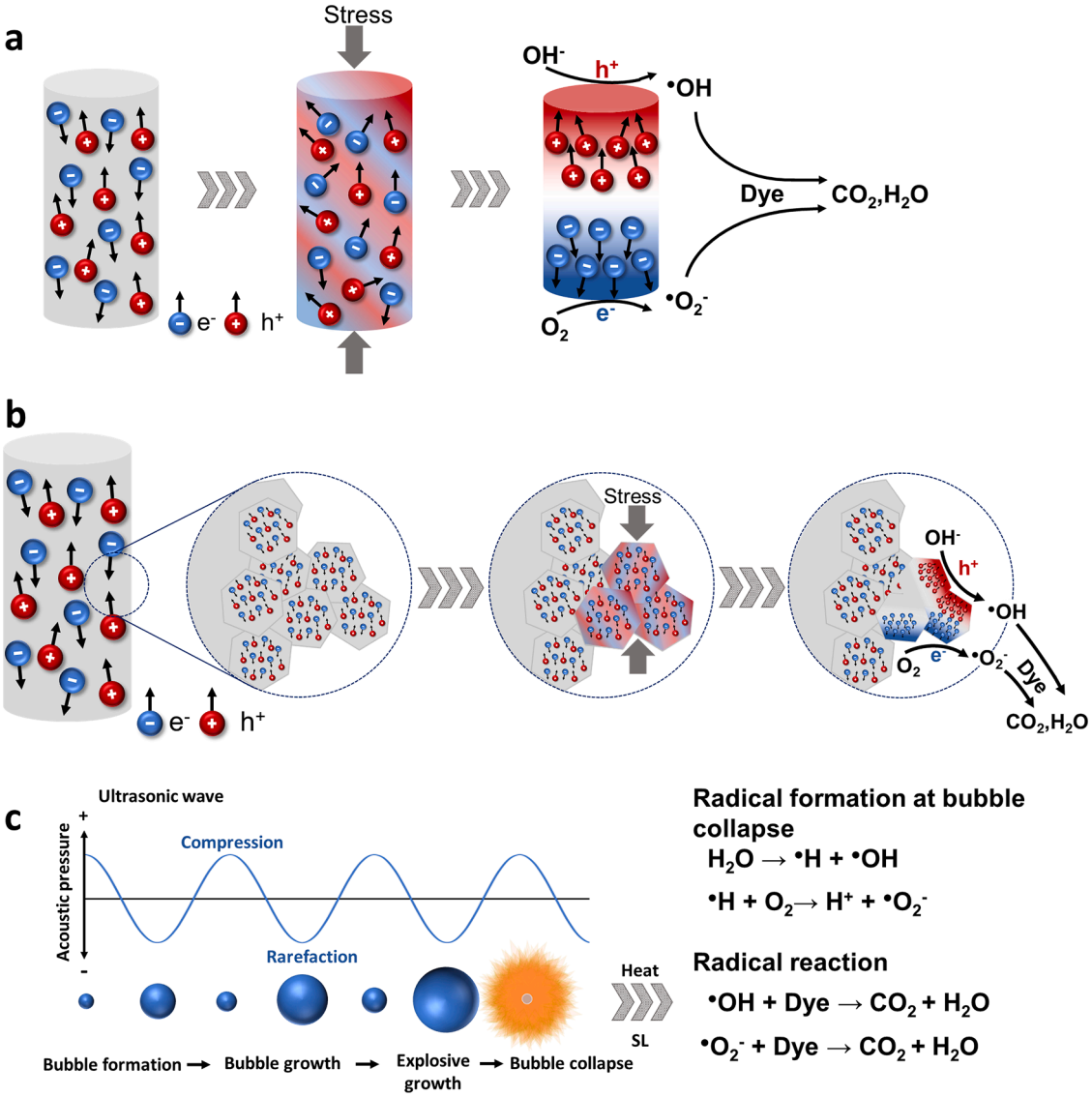

Fig. 1. Illustration of the different mechanisms for the overall piezocatalytic degradation of dyes: a) 'top-to-bottom' electric potential difference due to bulk polarisation of a piezoelectric particle under stress, b) electric potential difference due to localised polarisation within micro- and nano-structured features of piezocatalysts, c) bubble formation, growth and collapse under ultrasound and resulting chemical processes (i.e. sonochemistry).

2. Experimental

2.1. Catalyst preparation and characterisation

The piezoelectric material (poled potassium bismuth titanate-bismuth ferrite lead titanate, BF-KBT-PT) [34,35] and procedure that had been previously developed by the authors [29] were again employed to fabricate the piezocatalysts used in this study. The reasons for choosing this material are several: the source material, when poled, is highly piezoelectric (d_{33} and d_{31} values of 100 pC/N and −40 pC/N, respectively). Its high coercive stress allows for the maintenance of the piezoelectric effect even after applied stress such as grinding and sieving into fine particles to make the piezocatalysts (<63 μm)[29]. Focused ion beam-scanning electron microscopy (FIB-SEM, Zeiss Crossbeam 550) with an energy dispersive X-ray spectrometer (EDS) was used to analyse the surface structure and composition, whereas X-ray powder diffraction (XRPD) data was collected using a Bruker D8 X-ray powder diffractometer with CuKα-radiation to determine the crystalline structure of the BF-KBT-PT catalysts. The presence of the piezoelectric effect in the BF-KBT-PT piezocatalysts was proven empirically using a Berlincourt metre (APC International) and aligning the unelectroded particles in the metre in various orientations.

2.2. Finite element simulations

A finite element method model previously developed by the authors coupling the acoustic field in the liquid with the vibration of a single piezocatalytic particle and its piezoelectric response was used to simulate BF-KBT-PT piezocatalysts freely suspended in a liquid (i.e. piezocatalyst/water mechanical system) to investigate their piezoelectric response between 20 and 1150 kHz. A detailed explanation of the model, its simplifications and advantages over other models employed in the literature, as well as the material properties defined, can be found in a previous work by the authors [29].

2.3. Experimental setups and procedure

As opposed to the general trend in the field based on the use of small reactors up to 100 mL [4,7,8,14,19], all the experiments included in this study were conducted in reactors with substantially larger working volumes of 500 and 1000 mL containing 5 mg L^{-1} Rhodamine B (RhB) aqueous solutions. Reactor/ultrasonic transducer position and operating parameters were carefully set and controlled, and acoustic power calibrations of various powers at all frequencies were conducted by the standard calorimetric calibration method [36], to ensure reproducibility and comparability of experiments carried out in the different experimental setups. This included the use of a precise temperature control system (Grant LT ecocool 100 recirculating chiller) to provide a constant operating temperature of 30 ± 2 °C throughout all the RhB degradation experiments. Samples of the RhB aqueous solutions (3 mL) were taken every 10 min with a 0.22 μm PTFE-syringe-filter. Samples were then analysed by ultraviolet–visible spectroscopy (Shimadzu UV-3600 Plus) at the characteristic wavelength of 554 nm. In the piezocatalytic degradation experiments, 0.001 g mL^{-1} of BF-KBT-PT piezocatalysts were added to the RhB aqueous solution. To ensure adsorption-desorption equilibrium was reached, RhB aqueous solution containing the appropriate amount of catalyst were stirred at 200 rpm for 30 min. As previously reported, no adsorption nor photocatalytic degradation of RhB took place throughout the experiments [29].

Additional experiments to confirm previously reported radical initiated degradation routes [6,29] at high and low ultrasonic frequencies for sonochemical and piezocatalytic degradation of RhB were conducted in the presence and absence of BF-KBT-PT piezocatalysts and several radical and charge scavengers: 10 mM terephthalic acid (TA), 10 mM benzoquinone (BQ) and 2 mM ethylenediaminetetraacetic acid (EDTA) disodium salt dihydrate, all of high purity (99.5%, 99% and 99+%, respectively) from ACROS Organics. TA, BQ and EDTA were selected due to their role as chemical traps for $^{\bullet}OH$ [37], $^{\bullet}O_2^-$ [38] and h^+ [39], respectively.

2.3.1. Low ultrasonic frequency setups

An ultrasonic horn (Branson SFX 550) was employed for the experiments conducted at 20 kHz (Fig. 2a). The ultrasonic horn was centred and immersed to a depth of 4 cm into in a 1000 mL double-jacketed batch reactor. Depending on the experimental condition, the acoustic power was adjusted and calibrated as follows: 12.4 ± 0.4, 38.1 ± 0.7, 50.1 ± 0.3, 68.0 ± 0.3 and 89.8 ± 0.4 W L^{-1}.

An ultrasonic bath (Ultrawave QS12) was used for the experiments carried out at 32-38 kHz (Fig. 2b). A 1000 mL beaker was centred and immersed to a depth of 4 cm into the ultrasonic bath with a constant water level. The ultrasonic bath was operated at a full calibrated power of 12.2 ± 0.4 W L^{-1}. Prior to each experiment, the water in the ultrasonic bath was thoroughly degassed for 60 min ensuring a reproducible acoustic field inside the bath.

2.3.2. High ultrasonic frequency setup

An ultrasonic power multifrequency generator (Meinhard Ultrasonics) equipped with a 500 mL long-neck flask was used to conduct the experiments at 576, 864 and 1142 kHz (Fig. 2c). The power was adjusted and calibrated depending on the experimental conditions. The calibrated acoustic powers were 2.9 ± 0.4, 5.5 ± 0.4, 10.6 ± 0.3, 20.3 ± 0.7 and 33.7 ± 0.6 W L^{-1} at 576 kHz, 11.0 ± 0.6 W L^{-1} at 864 kHz and 10.0 ± 0.7 W L^{-1} at 1142 kHz.

2.3.3. Aluminium foil erosion experiments

The well-established aluminium foil erosion method [40–43] was performed to qualitatively evaluate the intensity of mechanical effects at different frequencies and power of 10-12 W L^{-1}. This method consisted of vertically suspending aluminium foil sheets within the reactor part of the different experimental setups used in this study. For this purpose, customised holders were designed and additive manufactured to secure the aluminium foil sheets within the reactors during the experiments. In all cases, the aluminium foil sheets were immersed in the sonicated solution for 5 min to allow for sufficient erosion of the foil.

3. Results and discussion

3.1. Catalyst characterisation

As reported in a previous work by the authors [29], FIB-SEM analysis revealed that the vast majority of BF-KBT-PT piezocatalysts exhibited a cuboid morphology with a particle size in the order of 63 μm or smaller (Fig. 3a). XRPD data (Fig. 3b) indicated peak splitting in the (200) phase; however, peak splitting of the (111) phase was not observed, confirming negligible lattice distortion of the rhombohedral phase due to the poled nature of the material [34]. XRPD data also confirmed the perovskite structure of BF-KBT-PT with no visible secondary phases [34]. Empiric piezoelectric analysis of BF-KBT-PT piezocatalysts in various random orientations (e.g. −35, −42, −47 or +143 pC/N) showed that the ground particles conserved their high piezoelectric nature (Fig. 3c).

3.2. Effect of ultrasonic frequency

3.2.1. FEM simulations

FEM simulations of a single BF-KBT-PT piezocatalyst suspended in water at ultrasonic frequencies ranging from 15 to 1150 kHz indicated the existence of six global resonance frequencies of the piezocatalyst/water mechanical system within the studied range (Fig. 4a): 123, 370, 618, 864, 1055 and 1111 kHz. In an ideal scenario, these are the frequencies the BF-KBT-PT piezocatalysts should be excited at, besides its resonance frequency (which would be in the MHz scale). However, in

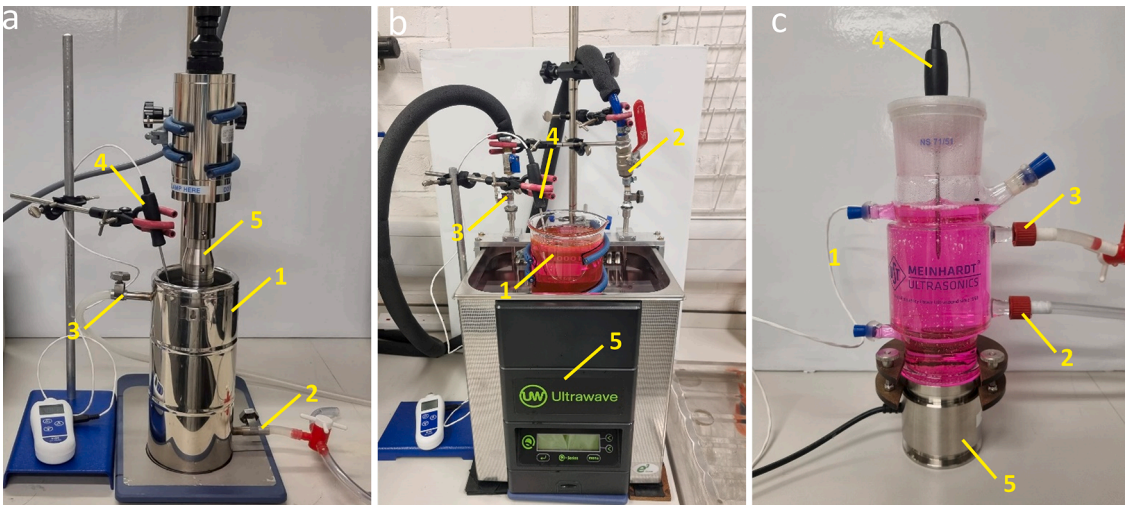

Fig. 2. Experimental setups used in the present study: a) 20 kHz ultrasonic horn setup, b) 32-38 kHz ultrasonic bath setup, c) 576, 864 and 1142 kHz multifrequency setup. Key components in all setups: 1) reactor, 2) cooling system inlet, 3) cooling system outlet, 4) thermocouple, 5) ultrasonic source.

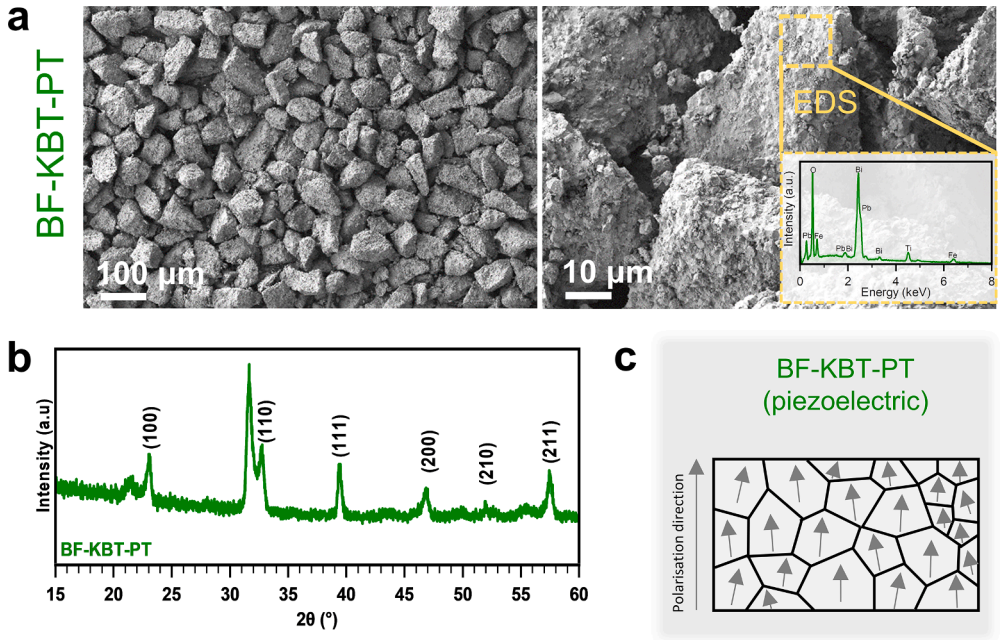

Fig. 3. Material characterisation of BF-KBT-PT piezocatalysts [29]: a) FIB-SEM and EDS, b) XRPD data. c) Schematic of aligned Weiss domains for piezoelectric BF-KBT-PT.

practice, the operating frequencies of ultrasonic systems depend upon the piezoceramics used to build the transducers that generate the acoustic field within the irradiated liquid, the liquid itself and the final geometry of the system [25,26,44]; operating frequencies are therefore close to the resonance frequency of the piezoceramics within the transducer that allow for its resonance in length mode [45]. For this reason, the simulated polarisation experienced by the piezocatalyst at the operating frequencies of the ultrasonic systems used in this study (20, 35, 576, 864 and 1142 kHz) were further investigated (Fig. 4b-f).

FEM simulations at 20, 35, 576, 864 and 1142 kHz indicated that, out of the five operating frequencies experimentally investigated in this study, 864 kHz (i.e. a global resonance frequency) should theoretically result in the BF-KBT-PT piezocatalyst achieving the greatest 'top-to-bottom' electric potential difference of 69.1 V. The minimum theoretical potential required for the redox reactions responsible of the piezocatalytic generation of $^{\bullet}OH$ and $^{\bullet}O_2^-$ radicals is 2.22 V (oxidation: $OH^- + h^+ \rightarrow {}^{\bullet}OH$, +1.89 V vs SHE [46]; Reduction: $O_2 + e^- \rightarrow {}^{\bullet}O_2^-$ [47]. Therefore, this theoretical result would in principle support the occurrence of bulk piezoelectric polarisation as a mechanism driving the piezocatalytic degradation of RhB at 864 kHz via $^{\bullet}OH$ and $^{\bullet}O_2^-$ radicals (Fig. 1a). At 576 and 1142 kHz, 'top-to-bottom' electric potential differences of 0.14 and 0.12 V, respectively, were observed. This would not be enough to overcome the minimum of 2.22 V by bulk polarisation, but other phenomena such as localised piezoelectric polarisation [48] (Fig. 1.b) or sonocatalysis [49] could still occur, resulting in the degradation of RhB by the same radicals, but to a lesser extent [29]. The latter would also apply to the low frequencies explored in this study, although to an even lesser extent, as the lowest 'top-to-bottom' electric potential difference of 0.08 V was observed for the simulations conducted at both 35 and 20 kHz.

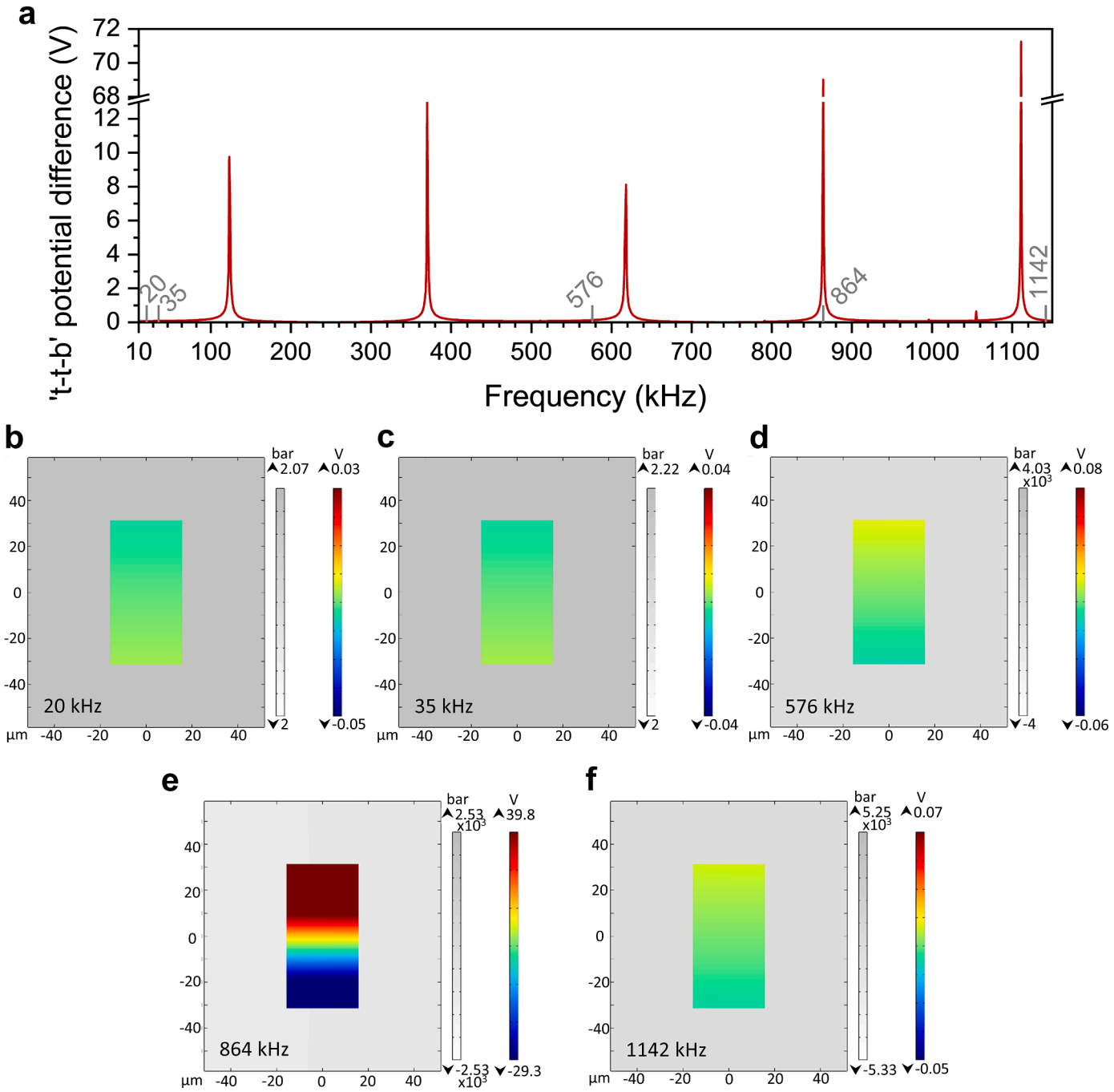

Fig. 4. a) 'Top-to-bottom' ('t-t-b') electric potential difference of a 63 μm BF-KBT-PT piezocatalyst suspended in water at ultrasonic frequencies ranging from 20 to 1150 kHz. b-f) 't-t-b' polarisation of a 63 μm BF-KBT-PT piezocatalyst suspended in water at different ultrasonic frequencies: 20, 35, 576, 864 and 1142 kHz, respectively.

3.2.2. RhB degradation experiments

Following the FEM simulations conducted at 20, 35, 576, 864 and 1142 kHz, one would expect to observe the greatest piezocatalytic effect at 864 kHz due to the greatest 'top-to-bottom' electric potential difference of 69.1 V observed at that global resonance frequency. However, RhB degradation experiments conducted at those same frequencies provided a completely different scenario (Fig. 5), even though the experiments indeed demonstrated the strong influence that frequency may have on the overall degradation of RhB. One reason for the disparity between the FEM simulations and the experimental results would be the simplifications made in the FEM model [29]: (i) use of 2D geometries (instead of 3D), (ii) use of linear acoustics not accounting for asymmetrical bubble collapses near the surface of the catalyst, (iii) the definition of perfectly smooth surfaces in the solid with no roughness that could result in localised piezoelectric polarisation and, especially, (iv) the simplified geometry of the domains used (i.e. small portion of liquid with a single piezocatalyst instead of the whole reactor with liquid and several hundreds or thousands of solid particles suspended in the liquid) . Another reason is related the acoustic pressure source defined in the FEM simulations (2 bar). Whilst 2 bar reflect a realistic acoustic pressure at low ultrasonic frequencies such as the 20 kHz ultrasonic horn or the 32-38 kHz ultrasonic bath [50–52], it may be too high for state-of-the-art systems operating at higher ultrasonic frequencies. This means that it is not possible, with state-of-the-art technology, to conduct

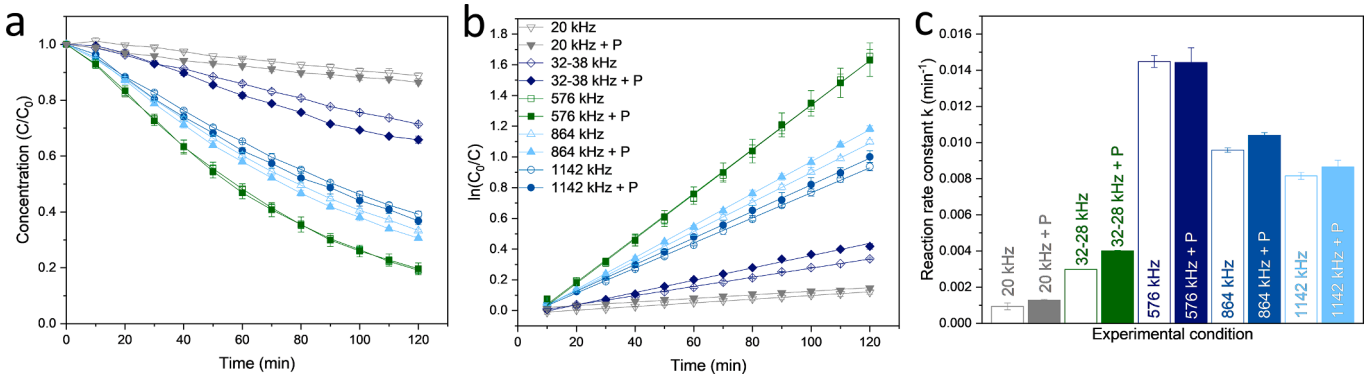

Fig. 5. RhB degradation experiments in the presence and absence of BF-KBT-PT piezocatalysts (P) at different frequencies and acoustic powers of 10-12 W $L-1$: a) evolution of C/C0 vs reaction time, b) pseudo first-order linear fit of ln(C0/C) vs reaction time, c) pseudo first-order degradation reaction rate constants.

experiments over a wide range of frequencies with exactly the same acoustic pressure source.

This situation, which indeed complicates the evaluation of the effect of frequency in piezocatalysis in terms of acoustic energy due to the differences in terms of reactor geometry, volume and ultrasonic source [53], can be overcome by estimating the acoustic power dissipated in the solution containing the piezocatalysts through calibration by calorimetry [36,54], a well-established method in sonochemistry research that enables the comparison by taking into account all those differences in the experimental setup [53]. For this reason, all the RhB degradation experiments displayed in Fig. 5 were conducted at a calibrated acoustic power around 10-12 W L^{-1}, as it was the maximum acoustic power that could be achieved by the 32-38 kHz ultrasonic bath; the dissipated acoustic powers in the different systems used at 20, 32–38, 576, 864 and 1142 kHz were 12.4 ± 0.4, 12.2 ± 0.4, 10.6 ± 0.3, 11.0 ± 0.6 and 10.0 ± 0.7 W L^{-1}, respectively.

RhB degradation experiments clearly showed two trends:

- At low frequencies, overall RhB degradation was rather low. In absence of the piezocatalyst (i.e. sonochemical generation of radicals only) [29], RhB degradations of around 11% and 29% were achieved at 20 and 32-38 kHz, respectively. The addition of the BF-KBT-PT piezocatalyst did result in a relative improvement of the overall degradation process, as RhB degradations of 14% (27% relative improvement) and 35% (21% relative improvement) were observed at 20 and 32-38 kHz, respectively.
- At higher frequencies, however, the overall degradation was significantly higher. In absence of the piezocatalyst, the greatest RhB degradation (81%) was observed at 576 kHz, whereas experiments conducted at 864 kHz and 1142 kHz yielded RhB degradations of 67% and 61%, respectively. In these cases, though, the addition of the BF-KBT-PT piezocatalyst did not result in a significant change in performance, as RhB degradations of 80% (0% relative improvement), 69% (3% relative improvement) and 63% (3% relative improvement) were observed at 576, 864 and 1142 kHz, respectively.

These results show that, when the ultrasonic frequency was varied from 20 to 1142 kHz while keeping the same acoustic power (around 10-12 W L^{-1}), the highest RhB was achieved at 576 kHz. This should not be a complete surprise, as it is believed that sonochemical radical formation is maximised at ultrasonic frequencies around 400 kHz [55–60]. Due to the shorter time length of the acoustic cycle, higher ultrasonic frequencies (>100 kHz) generally result in increased nucleation and a larger amount of cavitation bubbles that are smaller than at lower ultrasonic frequencies (i.e. 20-100 kHz) at the same acoustic power [30,31]. This results in enhanced formation of radicals [61] that contribute to the sonochemical degradation of RhB [29]. However, as also demonstrated by the present results, there is an upper limit of the applied ultrasonic frequency above which the RhB degradation diminishes, which is why RhB degradation at 864 and 1142 kHz was lower than that at 576 kHz. This is due to the bubbles forming at higher ultrasonic frequencies not being sufficiently large to undergo a violent collapse, hence why less radicals are formed to degrade RhB [30,53]. On the other hand, at lower ultrasonic frequencies (i.e. <100 kHz), cavitating bubbles are able to grow for longer time due to the longer time length of the acoustic cycle. As they grow larger, the bubbles undergo more violent collapses, resulting in less chemical effects like sonochemical formation of radicals [30,53], but more pronounced mechanical effects such as shock waves, micro-jetting and asymmetrical bubble collapse at the surface of solids [62].

To confirm the relevance of mechanical effects occurring at different frequencies used in this study, a qualitative evaluation of the acoustic field was conducted by immersing aluminium foil in the different experimental setups (Fig. 6). At low ultrasonic frequencies (<100 kHz), the aluminium foil experienced significant erosion caused by the mechanical effects of acoustic cavitation (Fig. 6a). This was particularly obvious for the foil immersed in the system operating at 32-38 kHz, where the greatest amount of erosion was observed. In fact, the erosion patterns clearly described the nature of the acoustic field established in the reactor, illustrating the clear existence of at least five pressure antinodes within the beaker where cavitating bubbles would concentrate. On the other hand, no noticeable erosion marks were observed by the naked eye on aluminium foil immersed in the multifrequency system operating at high frequencies (>100 kHz), a very clear indication of negligible mechanical effects (Fig. 6b). These results clearly link the occurrence of mechanical effects within the liquid being treated with the relative importance of the piezocatalytic contribution towards the degradation of RhB at different frequencies.

But why are mechanical effects generated by acoustic cavitation important in piezocatalysis? As previously stated, mechanical effects include phenomena such as shock waves, micro-jetting and, especially in this case, asymmetrical bubble collapse at the surface of solids. These phenomena result in piezocatalysts experiencing significantly high pressures (of the order of 100 bar), which would obviously lead to outstanding polarisations. The polarisation experienced by the piezocatalysts caused by the action of, for example, asymmetrical bubble collapses at their surface, would probably be far higher than the potential differences reported in the FEM simulations at low frequencies (<100 kHz); this polarisation would be enough to drive redox reactions at the surface of the piezocatalysts [63]. This is exactly the case of the present study, where the combination of a more violent collapse of cavitating bubbles with the poor sonochemical degradation of RhB via radical formation at low frequencies (<100 kHz) meant that, when BF-KBT-PT piezocatalysts were added to RhB aqueous solutions, a piezocatalytic contribution towards the degradation of RhB could be

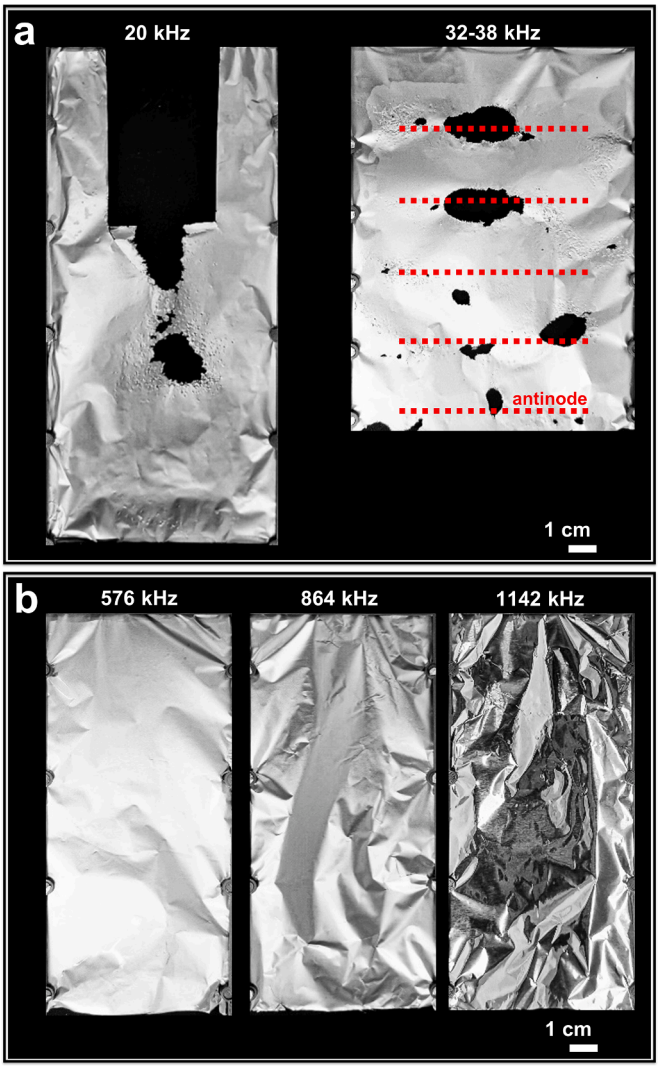

Fig. 6. Longitudinal view of aluminium foil erosion experiments (exposure time 5 min): a) low frequencies, b) high frequencies.

noticed. On the other hand, the superior sonochemical degradation of RhB via radical formation and the less violent collapse of cavitating bubbles at high ultrasonic frequencies (>100 kHz) [61] also explains why any potential piezocatalytic contribution is barely noticed in those conditions. In this case, though, the occurrence of mechanical effects that could cause a localised piezoelectric response [48] (Fig. 1b) would be more important than bulk piezoelectric polarisation resulting from exciting a piezocatalyst close to its resonance frequency (Fig. 1a). This was further confirmed by exploring the surface of the piezocatalysts after the experiments by FIB-SEM: in the particular case of the piezocatalysts used in experiments conducted at 32-38 kHz, smoother surfaces and erosion marks caused by asymmetric bubble collapses could be clearly seen (Fig. 7); a strong localised piezoelectric response would indeed be expected in the surroundings of those areas.

To summarise these findings, it can be stated that, with current ultrasonic transducer technology, one should focus in low ultrasonic frequencies to exploit the piezocatalytic degradation route to maximise the mechanical effects of acoustic cavitation; these would result in a localised piezoelectric response of the piezocatalyst (Fig. 1b). On the other hand, high frequencies would favour the sonochemical route (Fig. 1c), with no need to add a piezocatalyst at all.

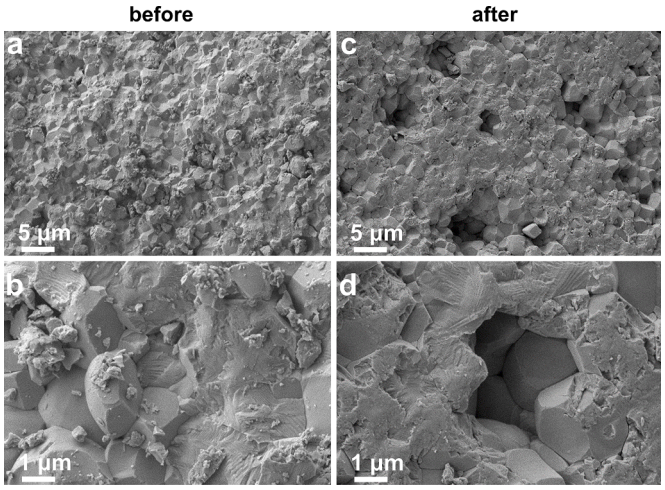

Fig. 7. FIB-SEM images of the surface of the BF-KBT-PT piezocatalyst used in experiments conducted at 32–38 kHz: a-b) before the experiment, c-d) after the experiment.

3.3. *Effect of ultrasonic power*

As demonstrated in the previous section, frequency is really important in both piezocatalytic and sonochemical degradation of RhB. Besides frequency, the other key parameter in ultrasonic systems is power. Therefore, to investigate the effect of ultrasonic power on both degradation mechanisms, additional experiments were conducted at 20 and 576 kHz. On the one hand, 20 kHz was chosen to investigate the effect of power at low ultrasonic frequencies for practical reasons: whereas the power output of the 20 kHz ultrasonic transducer could be further increased, the 32-38 kHz ultrasonic bath was already operating at its maximum power output. On the other hand, 576 kHz was chosen to investigate the effect of power at high ultrasonic frequencies due to the highest sonochemical degradation of RhB reported in the previous section.

Prior to the experiments, calorimetric calibrations were conducted at 20 and 576 kHz to determine five different acoustic power levels. At 20 kHz, the following acoustic powers were investigated based on the maximum output provided by the system: 12.4 ± 0.4, 38.1 ± 0.7, 50.1 ± 0.3, 68.0 ± 0.3 and 89.8 ± 0.4 W L^{-1}. At 576 kHz, the following acoustic powers were used, also based on the maximum output of the equipment: 2.9 ± 0.4, 5.5 ± 0.4, 10.6 ± 0.3, 20.3 ± 0.7 and 33.7 ± 0.6 W L^{-1}.

3.3.1. *Low ultrasonic frequency*

RhB degradation experiments conducted at 20 kHz (Fig. 8) revealed an increase in the overall degradation of RhB as the acoustic power was increased. RhB degradation in absence/presence of the BF-KBT-PT piezocatalyst was 11%/14% at 12 W L^{-1} (3% difference in overall degradation), 33%/37% at 38 W L^{-1} (4% difference in overall degradation) and 53%/64% at 50 W L^{-1} (11% difference in overall degradation), respectively, indicating a progressively growing contribution of piezocatalysis to the overall degradation of RhB. However, RhB degradation in the absence/presence of the BF-KBT-PT piezocatalyst was 79%/84% at 68 W L^{-1} (5% difference in overall degradation) and 92%/94% at 90 W L^{-1} (2% difference in overall degradation), indicating that, at certain point, further increasing the acoustic power would result in higher sonochemical degradation of RhB, but the contribution of the piezocatalyst towards the overall degradation would progressively decrease.

The apparent contradiction of these results can be explained with the effect of high ultrasonic power on the behaviour and distribution of cavitating bubbles at low frequencies, as illustrated by additional aluminium foil erosion experiments conducted in the 20 kHz setup at

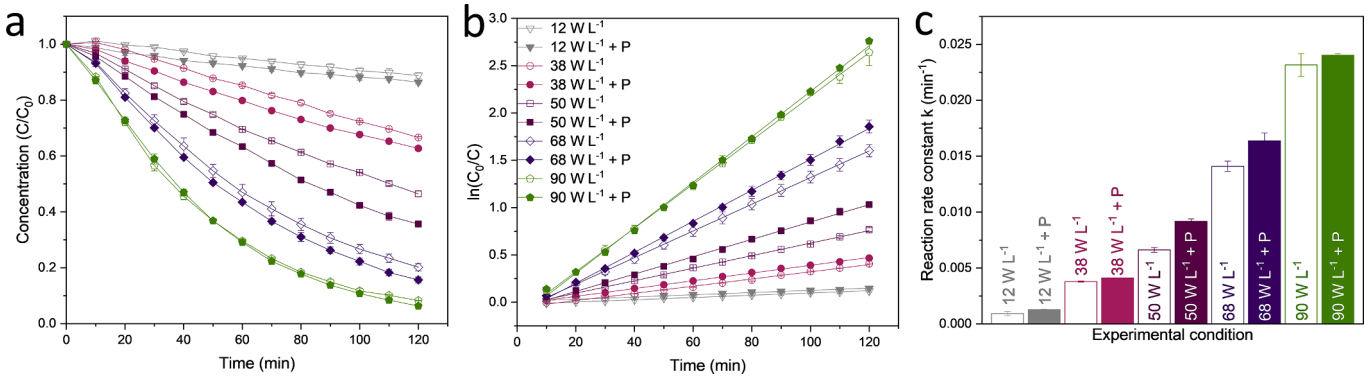

Fig. 8. RhB degradation experiments in the presence and absence of BF-KBT-PT piezocatalysts (P) at low frequency (20 kHz) and different acoustic powers: a) evolution of C/C0 vs reaction time. b) pseudo first-order linear fit of ln(C0/C) vs reaction time. c) pseudo first-order degradation reaction rate constants.

different acoustic powers (Fig. 9). As it is well known, there are upper and lower limits for acoustic power to result in 'efficient' cavitation activity [30,64]. Below the lower power threshold, the sound field is not efficient enough to induce bubble formation or nucleation; bubbles tend to succumb to surface tension effects and dissolve, leading to low cavitation activity [30,65]. This low cavitation activity would result in low sonochemical radical formation, but also low mechanical effects (Fig. 9a), hence the low sonochemical degradation and piezocatalytic contribution at 12 W L^{-1}. In between the upper and lower thresholds, the acoustic pressure influences not only the magnitude of the bubble collapse, but also the surface stability of the bubble as well as its oscillation. A more violent collapse results from the bubbles being exposed to higher negative pressures during the rarefaction phase of an ultrasonic wave, followed by higher pressures in the subsequent compression. This also leads to higher potential energy that is partially converted into radical formation, heat (i.e. higher collapse temperature), light (i.e. sonoluminescence) and sound emissions [58], with the subsequent increase in mechanical effects (Fig. 9b and c), hence the increase in sonochemical degradation and growing piezocatalytic contribution observed at 38 and, especially,50 W L^{-1}, where we can clearly see the piezocatalytic contribution of by the BF-KBT-PT particles. However, at excessive acoustic powers, an increase in bubble coalescence, degassing and liquid agitation takes place [30,31]. These phenomena may not have been enough to negatively affect the sonochemical degradation observed at 68 and 90 W L^{-1} (the overall degradation of RhB continued to increase), but it had a progressively negative effect on the mechanical effects that affect piezocatalysis (Fig. 9d and especially e), resulting in lower piezocatalytic contribution at 68 and 90 W L^{-1}. This did not mean that the acoustic field was weaker at those acoustic powers, though; in fact, the presence of a stronger pressure antinode could be noticed far from the emitter surface at those two powers. Therefore, with current ultrasonic transducer technology, low ultrasonic frequencies at moderate powers should be the aim to maximise the piezocatalytic degradation route, as high powers could result in a decrease in piezocatalytic activity.

Moreover, radical and charge scavenger experiments (Fig. 10) using TA, BQ and EDTA were conducted at 20 kHz and 50 W L^{-1} in the presence and absence of BF-KBT-PT piezocatalysts to further confirm the importance of radical initiated degradation routes in the degradation of RhB. TA showed a negligible effect on the sonochemical degradation of RhB at 20 kHz (Fig. 10a-c), indicating that $^{\bullet}$OH radicals were not being predominantly formed at such frequency and power. However, in the presence of BF-KBT-PT piezocatalysts, TA showed a more significant hindering effect on the overall degradation of RhB, suggesting the piezocatalytic formation of $^{\bullet}$OH in the presence of the piezocatalyst. BQ had a significant hindering effect on RhB degradation, whether in

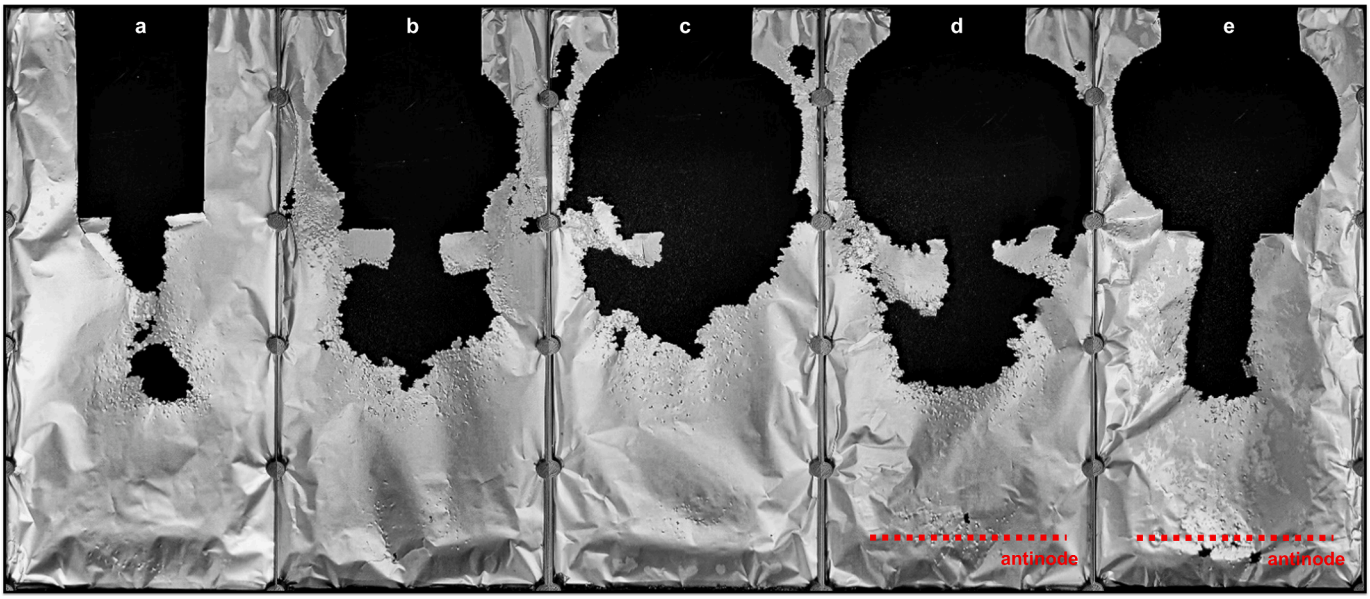

Fig. 9. Longitudinal view of aluminium foil erosion experiments (exposure time 5 min) conducted at low frequency (20 kHz) and different acoustic powers: a) 12 W $L-1$, b) 38 W $L-1$, c) 50 W $L-1$, d) 68 W $L-1$, e) 90 W $L-1$.

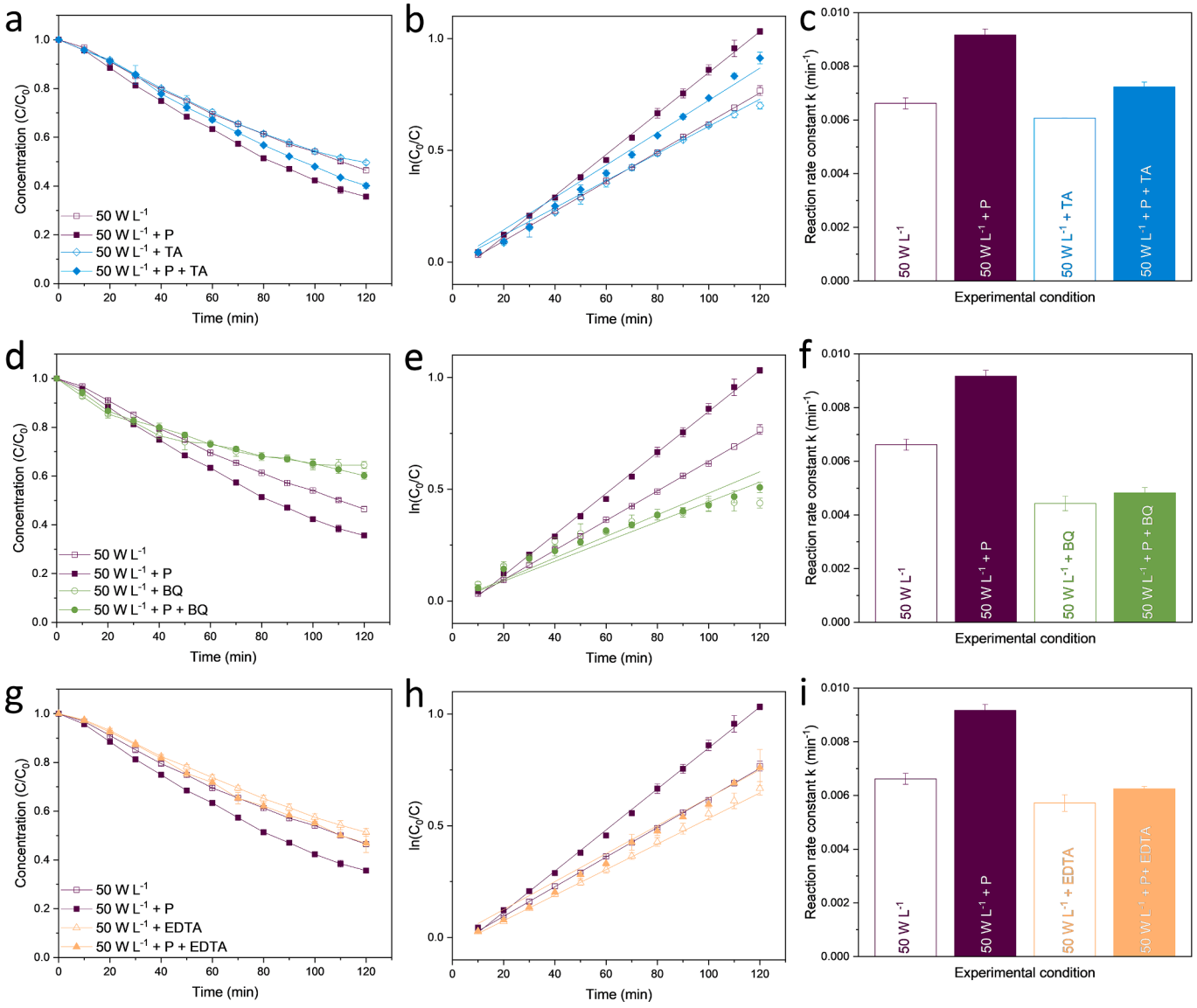

Fig. 10. RhB degradation experiments in the presence and absence of BF-KBT-PT piezocatalysts (P) at low frequency (20 kHz) and 50 W $L-1$ with different radical scavengers: a) evolution of C/C0 vs reaction time, b) pseudo first-order linear fit of ln(C0/C) vs reaction time, c) pseudo first-order degradation reaction rate constants in the presence of terephthalic acid (TA); d) evolution of C0/C vs reaction time, e) pseudo first-order linear fit of ln(C0/C) vs reaction time, f) pseudo first-order degradation reaction rate constants in the presence of benzoquinone (BQ); g) evolution of C0/C vs reaction time, h) pseudo first-order linear fit of ln(C0/C) vs reaction time, i) pseudo first-order degradation reaction rate constants in the presence of ethylenediaminetetraacetic acid (EDTA).

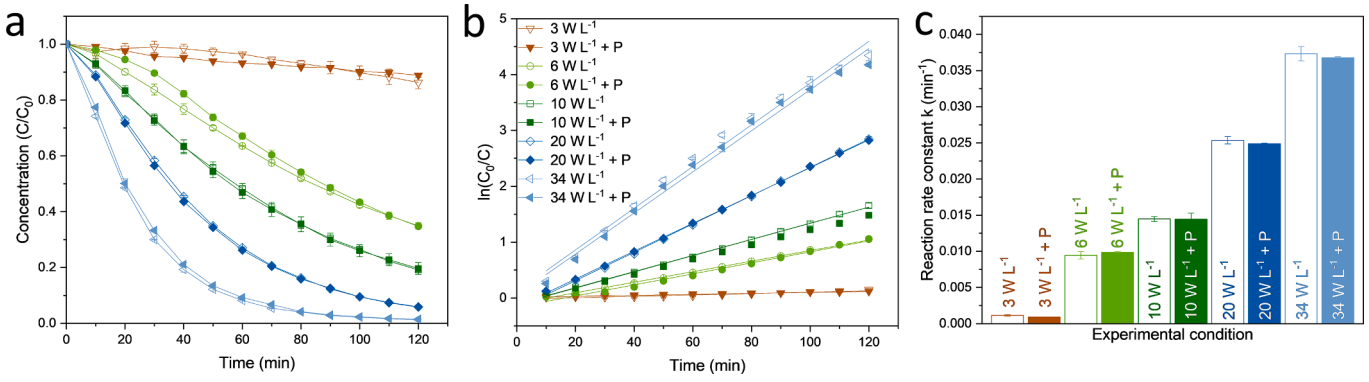

Fig. 11. RhB degradation experiments in the presence and absence of BF-KBT-PT piezocatalysts (P) at high frequency (576 kHz) with different acoustic powers: a) evolution of C/C0 vs reaction time. b) pseudo first-order linear fit of ln(C0/C) vs reaction time. c) pseudo first-order degradation reaction rate constants.

presence or absence of BF-KBT-PT piezocatalysts (Fig. 10D-f), demonstrating the importance of $^{\bullet}O_2^-$ radicals for the decomposition of RhB at low ultrasonic frequencies. The results also revealed that piezocatalytic degradation was significantly hindered using BQ to scavenger $^{\bullet}O_2^-$ radicals, indicating an enhanced production of $^{\bullet}O_2^-$ radicals in the presence of BF-KBT-PT piezocatalysts at the selected frequency and power. EDTA showed some minor decrease in the sonochemical degradation of RhB (Fig. 10g-i) due to its potential interaction with sonochemical formation of radicals [29,66]. However, the scavenging effect of EDTA on h^+ was clearly noticeable in the presence of BF-KBT-PT piezocatalysts, reducing the overall degradation of RhB close to the sonochemical decomposition. This demonstrates the importance of h^+ in the piezocatalytic degradation at lower ultrasonic frequencies.

3.3.2. *High ultrasonic frequency*

RhB degradation experiments conducted at 576 kHz (Fig. 11) also showed a progressive enhancement of the sonochemical degradation of RhB as the ultrasonic power was increased: overall RhB degradations of 14%, 65%, 80% and 94% were achieved at 3, 6, 10 and 20 W L^{-1}, respectively. Moreover, at the highest acoustic power used (34 W L^{-1}), 99% of RhB was degraded after 110 min; in other words, almost complete degradation of RhB was achieved in less than 2 h. As expected from the results from the previous section, the addition of the BF-KBT-PT piezocatalysts had little to no effect on the overall degradation, further indicating that only sonochemical degradation (Fig. 1c) with no piezocatalytic contribution was taking place at 576 kHz, no matter which acoustic power was being used. This should not be a complete surprise, though; near complete sonochemical degradation of RhB after 2-hour experiments at 300 kHz has been reported in the past, although at powers apparently higher (around 200 W L^{-1}) [67] than those reported in this study.

To better understand the observed degradation of RhB at higher ultrasonic frequencies, radical and charge scavenger experiments using TA, BQ and EDTA were again conducted at 576 kHz and 34 W L^{-1} (Fig. 12). TA showed some hindering effect on the degradation performance in the first 60 min of the experiments both in the absence and

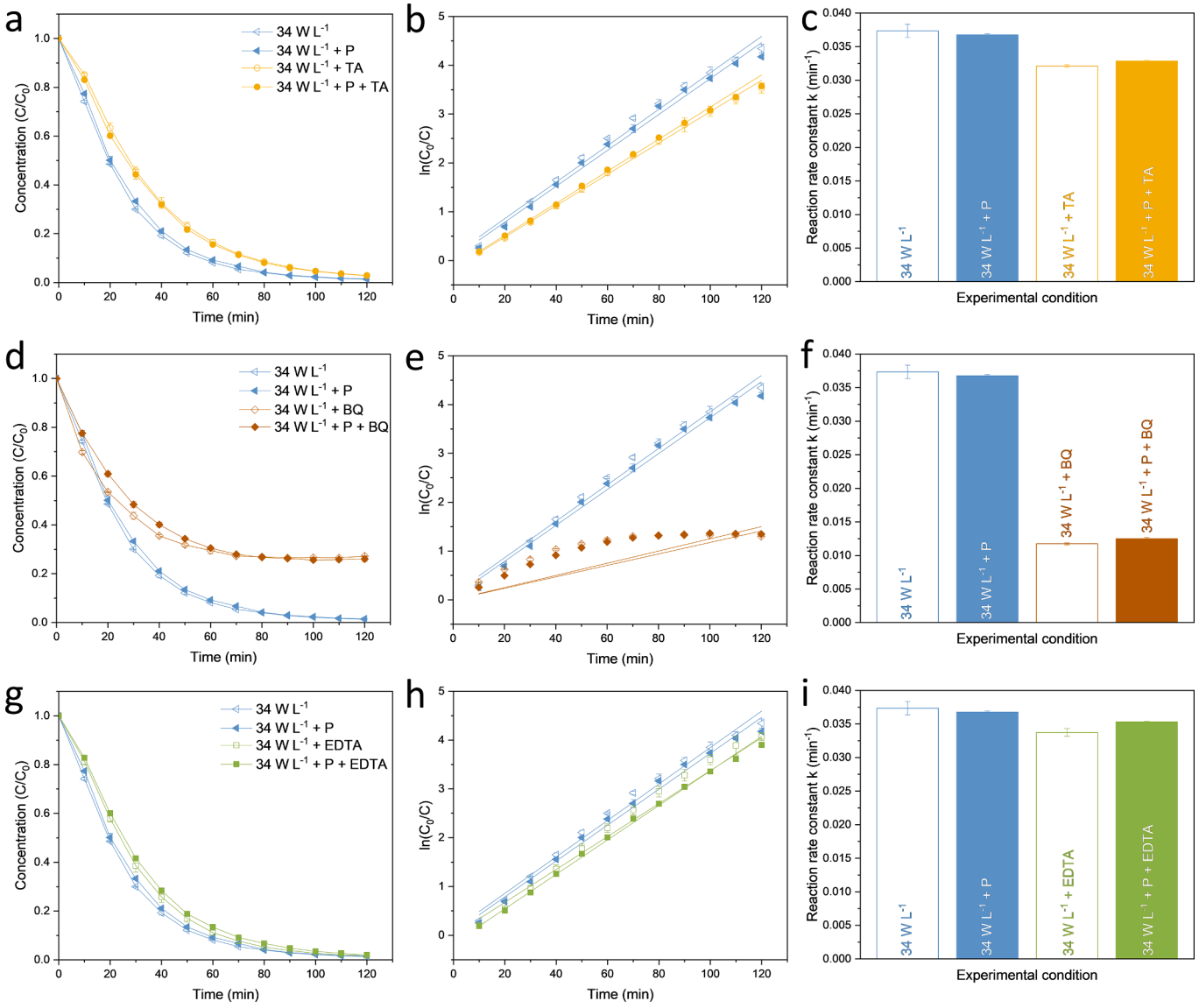

Fig. 12. RhB degradation experiments in the presence and absence of BF-KBT-PT piezocatalysts (P) at high frequency (576 kHz) and 34 W $L-1$ with different radical scavengers: a) evolution of C/C0 vs reaction time, b) pseudo first-order linear fit of ln(C0/C) vs reaction time, c) pseudo first-order degradation reaction rate constants in the presence of terephthalic acid (TA); d) evolution of C0/C vs reaction time, e) pseudo first-order linear fit of ln(C0/C) vs reaction time, f) pseudo first-order degradation reaction rate constants in the presence of benzoquinone (BQ); g) evolution of C0/C vs reaction time, h) pseudo first-order linear fit of ln(C0/C) vs reaction time, i) pseudo first-order degradation reaction rate constants in the presence of ethylenediaminetetraacetic acid (EDTA).

presence of BF-KBT-PT piezocatalysts (Fig. 12a-c). However, due to the significantly greater formation of $^{\bullet}OH$ radicals at 576 kHz compared to that at 20 kHz (in agreement with previous studies[68]), the added concentration of 10 mM TA was not enough to hinder the degradation of RhB at the end of the experiment (10 mM was around the saturation point in the solution). Nevertheless, the hindering effect was noticeable enough to confirm the contribution of $^{\bullet}OH$ radicals towards the degradation of RhB at high frequencies. The addition of BQ resulted in a significant hindering effect of the degradation of RhB (Fig. 12d-f) at 576 kHz, confirming the importance of $^{\bullet}O_2^-$ radicals on the decomposition of RhB at high frequencies. The addition of EDTA, however, had a very minor effect in the degradation of RhB (Fig. 12g-i), and the minor effect observed was likely due to the potential interaction of EDTA with the sonochemical formation of radicals [29,66]. The results in the presence of the BF-KBT-PT piezocatalysts are particularly revealing, confirming that h^+ were not involved in the degradation of RhB at 576 kHz. In other words, it further confirmed that there was no piezocatalysis taking place at high ultrasonic frequencies.

3.4. Overall discussion

The results from the experiments conducted at both low and high frequencies bring up an interesting discussion. At 20 kHz, whereas the presence of BF-KBT-PT piezocatalysts did enhance the overall degradation of RhB at 50 W L^{-1} (RhB degradation of 53%/64% in presence/absence of the piezocatalyst), further increasing the power to 90 W L^{-1} would result in a significantly higher RhB degradation with little contribution from the BF-KBT-PT piezocatalysts (RhB degradation of 92%/94% in the presence/absence of the piezocatalyst). In both cases, the piezocatalyst contribution would be strongly related to the mechanical effects caused by acoustic cavitation (e.g. shock waves, micro-jetting and asymmetrical bubble collapses near the surface of the piezocatalyst) that are maximised at low frequencies (<100 kHz). These mechanical effects might not be enough to generate by bulk polarisation (Fig. 1a) the minimum of 2.22 V necessary for the radical redox reactions to take place, but more than enough to cause localised piezoelectric polarisation (Fig. 1b) that would induce those reactions. Considering the energy requirements for ultrasound to generate acoustic cavitation and the resulting mechanical effects at low frequencies, though, one might prefer to explore less energy intensive options such as water-drive piezo-activation to achieve localised polarisation of piezocatalysts [69,70]. On the other hand, whereas no piezocatalysis was observed at high frequencies (>100 kHz) due to the significant decrease in the intensity and violence of those same mechanical effects, further tuning the frequency and increasing the power could result in the complete degradation of RhB at 576 kHz and 34 W L^{-1} through sonochemistry on its own (Fig. 1c). This would present straightforward advantages: there would be no need to add a catalyst to achieve the degradation (i.e. savings in materials, fabrication costs, separation processes after treatment, etc.), and there could be potential savings in energy consumption of the process, as full degradation was achieved at significantly lower acoustic powers than those used at 20 kHz.

Nevertheless, even with no piezocatalytic contribution to the overall process, the remarkable sonochemical degradation of RhB at 576 kHz and 34 W L^{-1} (pseudo first-order degradation reaction rate constant of 0.037 min^{-1}) outperforms the vast majority of the research on recent piezocatalytic degradation of RhB available in the literature (Table 1). As already indicated in their previous work [29] and more recently highlighted by other researchers [6,71], to achieve 'true' progress in piezocatalysis, expertise and practice from other fields (i.e. piezoelectricity, acoustics, sonochemistry and electrochemistry), as well as a systematic experimental approach with appropriate control experiments, must be incorporated into the research conducted in this area. If this is not followed, there is a strong risk that piezocatalysis may be, sooner rather than later, forgotten about without fully exploiting its potential.

Table 1
Comparison of pseudo first-order reaction rate constants for sonochemical and piezocatalytic degradation of RhB from this work with other piezocatalysis studies available in the literature.

Piezocatalyst	Frequency [kHz]	Acoustic power [W L^{-1}]	Rate constant [min^{-1}]	Ref
None	20	50.1 ± 0.3	0.007	this study
	20	89.8 ± 0.4	0.023	this study
	576	20.3 ± 0.7	0.025	this study
	576	33.7 ± 0.6	0.037	this study
BF-KBT-PT	20	50.1 ± 0.3	0.009	this study
	20	89.8 ± 0.4	0.024	this study
	576	20.3 ± 0.7	0.025	this study
	576	33.7 ± 0.6	0.037	this study
$BaTiO_3$	40	n/a (360 W)	0.013	[13]
$(Bi_{1/2}Na_{1/2})TiO_3$	40	n/a (100 W)	0.013	[14]
$Na_{0.5}Bi_{0.5}TiO_3$ (nanoparticles)	40	n/a (150 W)	0.022	[15]
$_{0.5}BNT–_{0.5}BFO$	40	n/a (120 W)	0.0204	[18]
$Bi_2Fe_4O_9$ (nanoplates)	40	n/a (200 W)	0.01615	[11]
$Ba_{0.95}Ca_{0.05}Ti_{0.9}Sn_{0.1}O_3$ (micron-sized powders)	40	n/a (100 W)	0.0245	[12]
$(K_{0.5}Na_{0.5})_{0.94}Li_{0.06}NbO_3$-PDMS	40	n/a (180 W)	~0.014	[9]
Bi- MOFs (bismuth-based)	40	n/a (300 W)	~0.025	[10]
Natural clay-modified MWCNT/kaolinite/PVDF membrane	30±5	n/a (50 W)	0.040	[19]
$Bi_2Fe_4O_9$ NSs	40	n/a (480 W)	0.0186	[20]
$BaTiO_3$@TiO_2 nanowires	28	n/a (n/a)	0.007	[17]
	45	n/a (200 W)	0.08	
	80	n/a (200 W)	0.002	
	100	n/a (200 W)	0.001	

4. Conclusion

The present study aimed to shed some light into the controversial discussion surrounding the piezocatalytic mechanisms by investigating the effect of ultrasonic frequency and power on the 'top-to-bottom' polarisation of piezocatalyst. The results indicated that the occurrence of mechanical effects (i.e. shock waves, micro-jetting and asymmetric collapse at the surface of the catalysts) predominant at lower ultrasonic powers (<100 kHz) would cause a localised piezoelectric response that would be more important for current piezocatalytic research rather than bulk piezoelectric polarisation resulting from exciting a piezocatalyst close to its resonance frequency.

The results also revealed that, whilst an increase in acoustic power would result in increased sonochemical degradation at both low and high ultrasonic frequencies, it did not necessarily result in an increased piezocatalytic contribution. Therefore, the use of lower ultrasonic frequencies with moderate powers should be encourage to maximise the piezocatalytic degradation route, whereas high powers and especially high ultrasonic frequencies would be favourable for the sonochemical degradation without the need to add a piezocatalyst. The latter could present straightforward advantages: savings in cost of materials, their

fabrication and post-treatment separation, as well as potential energy consumption.

Funding information

School of Engineering, The University of Edinburgh – Start Up fund. Carnegie Trust for the Universities of Scotland – RIG009799 grant. EPSRC – EP/P030564/1 grant.

CRediT authorship contribution statement

Franziska Bößl: Conceptualization, Methodology, Validation, Formal analysis, Investigation, Data curation, Writing – original draft, Visualization. **Valentin C. Menzel:** Methodology, Investigation. **Efthalia Chatzisymeon:** Resources, Writing – review & editing. **Tim P. Comyn:** Resources, Writing – review & editing. **Peter Cowin:** Resources. **Andrew J. Cobley:** Resources, Writing – review & editing. **Ignacio Tudela:** Conceptualization, Methodology, Resources, Writing – review & editing, Supervision, Project administration, Funding acquisition.

Declaration of Competing Interest

The authors declare that they have no known competing financial interests or personal relationships that could have appeared to influence the work reported in this paper.

Data availability

Data will be made available on request.

Acknowledgements

FB and IT acknowledge the University of Edinburgh for funding this research through its Start Up fund. IT would also like to thank the Carnegie Trust for the Universities of Scotland for its support through the Research Incentive Grant scheme (RIG009799). The authors also acknowledge the use of the Zeiss Crossbeam 550 FIB-SEM funded with EPSRC grant EP/P030564/1, and would also like to thank Dr James Cumby and Dr Thomas Glenn at the University of Edinburgh for their kind support in XRD and FIB-SEM analysis, respectively, as well as Mr Gordon Paterson for his help with some of the experimental setups used in this study.

References

[1] K. Wang, C. Han, J. Li, J. Qiu, J. Sunarso, S. Liu, The mechanism of piezocatalysis: energy band theory or screening charge effect? Angew. Chem. Int. Ed Engl. 61 (6) (2022), e202110429 https://doi.org/10.1002/anie.202110429.

[2] K.-S. Hong, H. Xu, H. Konishi, X. Li, Direct water splitting through vibrating piezoelectric microfibers in water, J. Phys. Chem. Lett. 1 (6) (2010) 997–1002, https://doi.org/10.1021/jz100027t.

[3] K.-S. Hong, H. Xu, H. Konishi, X. Li, Piezoelectrochemical Effect: a new mechanism for azo dye decolorization in aqueous solution through vibrating piezoelectric microfibers, The J. Phys. Chem. C 116 (24) (2012) 13045–13051, https://doi.org/10.1021/jp211455z.

[4] E. Lin, Z. Kang, J. Wu, R. Huang, N. Qin, D. Bao, BaTiO3 nanocubes/cuboids with selectively deposited Ag nanoparticles: efficient piezocatalytic degradation and mechanism, Appl. Catal. B: Environ. 285 (2021), https://doi.org/10.1016/j.apcatb.2020.119823.

[5] A. Zhang, Z. Liu, B. Xie, J. Lu, K. Guo, S. Ke, L. Shu, H. Fan, Vibration catalysis of eco-friendly Na0.5K0.5NbO3-based piezoelectric: an efficient phase boundary catalyst, Appl. Catal. B: Environ. 279 (2020), https://doi.org/10.1016/j.apcatb.2020.119353.

[6] H. Kalhori, A.H. Youssef, A. Ruediger, A. Pignolet, Competing contributions to the catalytic activity of barium titanate nanoparticles in the decomposition of organic pollutants, J. Environ. Chem. Eng. 10 (6) (2022), https://doi.org/10.1016/j.jece.2022.108571.

[7] W. Ma, M. Lv, F. Cao, Z. Fang, Y. Feng, G. Zhang, Y. Yang, H. Liu, Synthesis and characterization of ZnO-GO composites with their piezoelectric catalytic and antibacterial properties, J. Environ. Chem. Eng. 10 (3) (2022), https://doi.org/10.1016/j.jece.2022.107840.

[8] X. Zhou, Q. Sun, Z. Xiao, H. Luo, D. Zhang, Three-dimensional BNT/PVDF composite foam with a hierarchical pore structure for efficient piezo-photocatalysis, J. Environ. Chem. Eng. 10 (5) (2022), https://doi.org/10.1016/j.jece.2022.108399.

[9] X. Cheng, Z. Liu, Q. Jing, P. Mao, K. Guo, J. Lu, B. Xie, H. Fan, Porous (K0.5Na0.5)0.94Li0.06NbO3-polydimethylsiloxane piezoelectric composites harvesting mechanical energy for efficient decomposition of dye wastewater, J. Colloid Interface Sci. 629 (Pt A) (2023) 11–21, https://doi.org/10.1016/j.jcis.2022.08.131.

[10] S. Dong, L. Wang, W. Lou, Y. Shi, Z. Cao, Y. Zhang, J. Sun, Bi-MOFs with two different morphologies promoting degradation of organic dye under simultaneous photo-irradiation and ultrasound vibration treatment, Ultrason Sonochem. 91 (2022), 106223, https://doi.org/10.1016/j.ultsonch.2022.106223.

[11] Y. Du, T. Lu, X. Li, Y. Liu, W. Sun, S. Zhang, Z. Cheng, High-efficient piezocatalytic hydrogen evolution by centrosymmetric Bi2Fe4O9 nanoplates, Nano Energy 104 (2022), https://doi.org/10.1016/j.nanoen.2022.107919.

[12] J. He, C. Yu, Y. Hou, X. Su, J. Li, C. Liu, D. Xue, J. Cao, Y. Su, L. Qiao, T. Lookman, Y. Bai, Accelerated discovery of high-performance piezocatalyst in BaTiO3-based ceramics via machine learning, Nano Energy 97 (2022), https://doi.org/10.1016/j.nanoen.2022.107218.

[13] Z. Hu, W. Dong, Z. Dong, P. Li, Q. Bao, T. Cao, Facile fabrication of tetragonal phase single-crystalline BaTiO3 terrace-like dendrite by a simple solvothermal method and its piezocatalytic properties, Mater. Chem. Phys. 293 (2023), https://doi.org/10.1016/j.matchemphys.2022.126911.

[14] D.-.M. Liu, J.-.T. Zhang, C.-.C. Jin, B.-.B. Chen, J. Hu, R. Zhu, F. Wang, Insight into oxygen-vacancy regulation on piezocatalytic activity of (Bi1/2Na1/2)TiO3 crystallites: experiments and first-principles calculations, Nano Energy 95 (2022), https://doi.org/10.1016/j.nanoen.2022.106975.

[15] L. Shi, C. Lu, L. Chen, Q. Zhang, Y. Li, T. Zhang, X. Hao, Piezocatalytic performance of Na0.5Bi0.5TiO3 nanoparticles for degradation of organic pollutants, J. Alloys Compd. 895 (2022), https://doi.org/10.1016/j.jallcom.2021.162591.

[16] X. Zhou, B. Shen, J. Zhai, N. Hedin, Reactive oxygenated species generated on iodide-doped BiVO4/BaTiO3 heterostructures with Ag/Cu nanoparticles by coupled piezophototronic effect and plasmonic excitation, Adv. Funct. Mater. 31 (13) (2021), https://doi.org/10.1002/adfm.202009594.

[17] Q. Liu, D. Zhai, Z. Xiao, C. Tang, Q. Sun, C.R. Bowen, H. Luo, D. Zhang, Piezo-photoelectronic coupling effect of BaTiO3@TiO2 nanowires for highly concentrated dye degradation, Nano Energy 92 (2022), https://doi.org/10.1016/j.nanoen.2021.106702.

[18] Z. Liu, Y. Zheng, S. Zhang, J. Fu, Y. Li, Y. Zhang, W. Ye, (1−x) Bi0.5Na0.5TiO3–xBiFeO3 solid solutions with enhanced piezocatalytic dye degradation, Sep. Purif. Technol. 290 (2022), https://doi.org/10.1016/j.seppur.2022.120831.

[19] D. Mondal, S. Bardhan, N. Das, J. Roy, S. Ghosh, A. Maity, S. Roy, R. Basu, S. Das, Natural clay-based reusable piezo-responsive membrane for water droplet mediated energy harvesting, degradation of organic dye and pathogenic bacteria, Nano Energy 104 (2022), https://doi.org/10.1016/j.nanoen.2022.107893.

[20] C. Su, C. Li, R. Li, W. Wang, Insights into highly efficient piezocatalytic molecule oxygen activation over Bi2Fe4O9: active sites and mechanism, Chem. Eng. J. 452 (2023), https://doi.org/10.1016/j.cej.2022.139300.

[21] P.L. Wang, X.Y. Li, S.Y. Fan, X. Chen, M.C. Qin, D. Long, M.O. Tad, S.M. Liu, Impact of oxygen vacancy occupancy on piezo-catalytic activity of BaTiO3 nanobelt, Appl. Catal. B-Environ. 279 (2020), https://doi.org/10.1016/j.apcatb.2020.119340.

[22] B. Yuan, J. Wu, N. Qin, E. Lin, Z. Kang, D. Bao, Sm-doped Pb(Mg1/3Nb2/3)O3-xPbTiO3 piezocatalyst: exploring the relationship between piezoelectric property and piezocatalytic activity, Appl. Mater. Today 17 (2019) 183–192, https://doi.org/10.1016/j.apmt.2019.07.015.

[23] F. Bößl, I. Tudela, Piezocatalysis: can catalysts really dance? Current Opinion in Green and Sustain. Chem. 32 (2021) https://doi.org/10.1016/j.cogsc.2021.100537.

[24] J. Wu, Q. Xu, E. Lin, B. Yuan, N. Qin, S.K. Thatikonda, D. Bao, Insights into the role of ferroelectric polarization in piezocatalysis of nanocrystalline BaTiO3, ACS Appl. Mater. Interfaces 10 (21) (2018) 17842–17849, https://doi.org/10.1021/acsami.8b01991.

[25] O. Louisnard, J. Gonzalez-Garcia, I. Tudela, J. Klima, V. Saez, Y. Vargas-Hernandez, FEM simulation of a sono-reactor accounting for vibrations of the boundaries, Ultrason. Sonochem. 16 (2) (2009) 250–259, https://doi.org/10.1016/j.ultsonch.2008.07.008.

[26] I. Tudela, V. Sáez, M.D. Esclapez, P. Bonete, H. Harzali, F. Baillon, J. González-García, O. Louisnard, Study of the influence of transducer-electrode and electrode-wall gaps on the acoustic field inside a sonoelectrochemical reactor by FEM simulations, Chem. Eng. J. 171 (1) (2011) 81–91, https://doi.org/10.1016/j.cej.2011.03.064.

[27] Y. Chen, S. Lan, M. Zhu, Construction of piezoelectric BaTiO3/MoS2 heterojunction for boosting piezo-activation of peroxymonosulfate, Chinese Chem. Lett. 32 (6) (2021) 2052–2056, https://doi.org/10.1016/j.cclet.2020.11.016.

[28] K. Fan, C. Yu, S. Cheng, S. Lan, M. Zhu, Metallic Bi self-deposited BiOCl promoted piezocatalytic removal of carbamazepine, Surfaces and Interfaces 26 (2021), https://doi.org/10.1016/j.surfin.2021.101335.

[29] F. Bößl, T.P. Comyn, P.I. Cowin, F.R. García-García, I. Tudela, Piezocatalytic degradation of pollutants in water: importance of catalyst size, poling and excitation mode, Chem. Eng. J. Adv. 7 (2021), https://doi.org/10.1016/j.ceja.2021.100133.

[30] R.J. Wood, J. Lee, M.J. Bussemaker, A parametric review of sonochemistry: control and augmentation of sonochemical activity in aqueous solutions, Ultrason Sonochem. 38 (2017) 351–370, https://doi.org/10.1016/j.ultsonch.2017.03.030.
[31] E.A. Serna-Galvis, J. Lee, F. Hernández, A.M. Botero-Coy, R.A. Torres-Palma, Sonochemical advanced oxidation processes for the removal of pharmaceuticals in wastewater effluents, Removal and Degradation of Pharmaceutically Active Compounds in Wastewater Treatment (2020) 349–381.
[32] Z. Eren, N.H. Ince, Sonolytic and sonocatalytic degradation of azo dyes by low and high frequency ultrasound, J. Hazard Mater. 177 (1–3) (2010) 1019–1024, https://doi.org/10.1016/j.jhazmat.2010.01.021.
[33] M.H. Abdurahman, A.Z. Abdullah, N.F. Shoparwe, A comprehensive review on sonocatalytic, photocatalytic, and sonophotocatalytic processes for the degradation of antibiotics in water: synergistic mechanism and degradation pathway, Chem. Eng. J. 413 (2021), https://doi.org/10.1016/j.cej.2020.127412.
[34] J. Bennett, A.J. Bell, T.J. Stevenson, T.P. Comyn, Tailoring the structure and piezoelectric properties of BiFeO3-(K0.5Bi0.5)TiO3–PbTiO3 ceramics for high temperature applications, Appl. Phys. Lett. 103 (15) (2013), https://doi.org/10.1063/1.4824652.
[35] T. Stevenson, D.G. Martin, P.I. Cowin, A. Blumfield, A.J. Bell, T.P. Comyn, P. M. Weaver, Piezoelectric materials for high temperature transducers and actuators, J. Mater. Sci. Mater. Electron. 26 (12) (2015) 9256–9267, https://doi.org/10.1007/s10854-015-3629-4.
[36] R.F. Contamine, A.M. Wilhelm, J. Berlan, H. Delmas, Power measurement in sonochemistry, Ultrason. Sonochem. 2 (1) (1995) S43–S47, https://doi.org/10.1016/1350-4177(94)00010-p.
[37] N. Wang, L. Zhu, M. Wang, D. Wang, H. Tang, Sono-enhanced degradation of dye pollutants with the use of H2O2 activated by Fe3O4 magnetic nanoparticles as peroxidase mimetic, Ultrason. Sonochem. 17 (1) (2010) 78–83, https://doi.org/10.1016/j.ultsonch.2009.06.014.
[38] J.M. Monteagudo, H. El-Taliawy, A. Duran, G. Caro, K. Bester, Sono-activated persulfate oxidation of diclofenac: degradation, kinetics, pathway and contribution of the different radicals involved, J. Hazard Mater. 357 (2018) 457–465, https://doi.org/10.1016/j.jhazmat.2018.06.031.
[39] S. Farhadi, F. Siadatnasab, A. Khataee, Ultrasound-assisted degradation of organic dyes over magnetic CoFe2O4@ZnS core-shell nanocomposite, Ultrason. Sonochem. 37 (2017) 298–309, https://doi.org/10.1016/j.ultsonch.2017.01.019.
[40] D. Krefting, R. Mettin, W. Lauterborn, High-speed observation of acoustic cavitation erosion in multibubble systems, Ultrason. Sonochem. 11 (3–4) (2004) 119–123, https://doi.org/10.1016/j.ultsonch.2004.01.006.
[41] N. Bretz, J. Strobel, M. Kaltenbacher, R. Lerch, Numerical simulation of ultrasonic waves in cavitating fluids with special consideration of ultrasonic cleaning, IEEE Ultrason. Symposium 2005 (2005) 703–706, https://doi.org/10.1109/ultsym.2005.1602948.
[42] M.M. Chivate, A.B. Pandit, Quantification of cavitation intensity in fluid bulk, Ultrason. Sonochem. 2 (1) (1995) S19–S25, https://doi.org/10.1016/1350-4177(94)00007-f.
[43] G. Servant, J.L. Laborde, A. Hita, J.P. Caltagirone, A. Gerard, Spatio-temporal dynamics of cavitation bubble clouds in a low frequency reactor: comparison between theoretical and experimental results, Ultrason. Sonochem. 8 (3) (2001) 163–174, https://doi.org/10.1016/s1350-4177(01)00074-8.
[44] I. Tudela, V. Saez, M.D. Esclapez, M.I. Diez-Garcia, P. Bonete, J. Gonzalez-Garcia, Simulation of the spatial distribution of the acoustic pressure in sonochemical reactors with numerical methods: a review, Ultrason. Sonochem. 21 (3) (2014) 909–919, https://doi.org/10.1016/j.ultsonch.2013.11.012.
[45] S. Sherrit, M. Badescu, A.C. Noell, F. Kehl, M.F. Mora, N.J. Oborny, J.S. Creamer, P. A. Willis, Acoustic processing of fluidic samples for planetary exploration, Front. Space Technol. 3 (2022), https://doi.org/10.3389/frspt.2022.752335.
[46] V.K. Sharma, Oxidation of inorganic contaminants by ferrates (VI, V, and IV)–kinetics and mechanisms: a review, J. Environ. Manag. 92 (4) (2011) 1051–1073, https://doi.org/10.1016/j.jenvman.2010.11.026.
[47] W.H. Koppenol, D.M. Stanbury, P.L. Bounds, Electrode potentials of partially reduced oxygen species, from dioxygen to water, Free Radic. Biol. Med. 49 (3) (2010) 317–322, https://doi.org/10.1016/j.freeradbiomed.2010.04.011.
[48] J. Zhang, C. Wang, C. Bowen, Piezoelectric effects and electromechanical theories at the nanoscale, Nanoscale 6 (22) (2014) 13314–13327, https://doi.org/10.1039/c4nr03756a.
[49] P. Qiu, B. Park, J. Choi, B. Thokchom, A.B. Pandit, J. Khim, A review on heterogeneous sonocatalyst for treatment of organic pollutants in aqueous phase based on catalytic mechanism, Ultrason. Sonochem. 45 (2018) 29–49, https://doi.org/10.1016/j.ultsonch.2018.03.003.
[50] R. Chow, R. Mettin, B. Lindinger, T. Kurz, W. Lauterborn, The importance of acoustic cavitation in the sonocrystallisation of ice - high speed observations of a single acoustic bubble, IEEE Symposium on Ultrasonics 2003 (2003) 1447–1450, https://doi.org/10.1109/ultsym.2003.1293177.
[51] D.J. Flannigan, K.S. Suslick, Plasma line emission during single-bubble cavitation, Phys. Rev. Lett. 95 (4) (2005), 044301, https://doi.org/10.1103/PhysRevLett.95.044301.
[52] K. Yasui, Influence of ultrasonic frequency on multibubble sonoluminescence, J. Acoust. Soc. Am. 112 (4) (2002) 1405–1413, https://doi.org/10.1121/1.1502898.
[53] T.J. Mason, A.J. Cobley, J.E. Graves, D. Morgan, New evidence for the inverse dependence of mechanical and chemical effects on the frequency of ultrasound, Ultrason. Sonochem. 18 (1) (2011) 226–230, https://doi.org/10.1016/j.ultsonch.2010.05.008.
[54] T. Kimura, T. Sakamoto, J.-.M. Leveque, H. Sohmiya, M. Fujita, S. Ikeda, T. Ando, Standardization of ultrasonic power for sonochemical reaction, Ultrason. Sonochem. 3 (3) (1996) S157–S161, https://doi.org/10.1016/s1350-4177(96)00021-1.
[55] M. Ashokkumar, J. Lee, S. Kentish, F. Grieser, Bubbles in an acoustic field: an overview, Ultrason. Sonochem. 14 (4) (2007) 470–475, https://doi.org/10.1016/j.ultsonch.2006.09.016.
[56] M.A. Beckett, I. Hua, Impact of Ultrasonic Frequency on Aqueous Sonoluminescence and Sonochemistry, The J. Phys. Chem. A 105 (15) (2001) 3796–3802, https://doi.org/10.1021/jp003226x.
[57] J.-.W. Kang, H.-.M. Hung, A. Lin, M.R. Hoffmann, Sonolytic Destruction of Methyl tert-Butyl Ether by Ultrasonic Irradiation: The Role of O3, H2O2, Frequency, and Power Density, Environ. Sci. Technol. 33 (18) (1999) 3199–3205, https://doi.org/10.1021/es9810383.
[58] P. Kanthale, M. Ashokkumar, F. Grieser, Sonoluminescence, sonochemistry (H2O2 yield) and bubble dynamics: frequency and power effects, Ultrason. Sonochem. 15 (2) (2008) 143–150, https://doi.org/10.1016/j.ultsonch.2007.03.003.
[59] S. Koda, T. Kimura, T. Kondo, H. Mitome, A standard method to calibrate sonochemical efficiency of an individual reaction system, Ultrason. Sonochem. 10 (3) (2003) 149–156, https://doi.org/10.1016/S1350-4177(03)00084-1.
[60] C. Petrier, A. Jeunet, J.L. Luche, G. Reverdy, Unexpected frequency effects on the rate of oxidative processes induced by ultrasound, J. Am. Chem. Soc. 114 (8) (2002) 3148–3150, https://doi.org/10.1021/ja00034a077.
[61] G. Portenlanger, H. Heusinger, The influence of frequency on the mechanical and radical effects for the ultrasonic degradation of dextranes, Ultrason. Sonochem. 4 (2) (1997) 127–130, https://doi.org/10.1016/s1350-4177(97)00018-7.
[62] K.V. Tran, T. Kimura, T. Kondo, S. Koda, Quantification of frequency dependence of mechanical effects induced by ultrasound, Ultrason. Sonochem. 21 (2) (2014) 716–721, https://doi.org/10.1016/j.ultsonch.2013.08.018.
[63] J. Wu, N. Qin, D. Bao, Effective enhancement of piezocatalytic activity of BaTiO3 nanowires under ultrasonic vibration, Nano Energy 45 (2018) 44–51, https://doi.org/10.1016/j.nanoen.2017.12.034.
[64] K.S. Suslick, Sonoluminescence and sonochemistry, in: 1997 IEEE Ultrasonics Symposium Proceedings. An International Symposium (Cat. No.97CH36118), 1997, pp. 523–532, https://doi.org/10.1109/ultsym.1997.663076.
[65] T.J. Matula, J.R. Blake, Inertial cavitation and single–bubble sonoluminescence, Philosophical Trans. Royal Soc. London. Series A: Math. Phys. Eng. Sci. 357 (1751) (1999) 225–249, https://doi.org/10.1098/rsta.1999.0325.
[66] L. Parizot, T. Chave, M.-.E. Galvez, H. Dutilleul, P. Da Costa, S.I. Nikitenko, Sonocatalytic oxidation of EDTA in aqueous solutions over noble metal-free Co3O4/TiO2 catalyst, Appl. Catal. B: Environ. 241 (2019) 570–577, https://doi.org/10.1016/j.apcatb.2018.09.001.
[67] S. Merouani, O. Hamdaoui, F. Saoudi, M. Chiha, Sonochemical degradation of Rhodamine B in aqueous phase: effects of additives, Chem. Eng. J. 158 (3) (2010) 550–557, https://doi.org/10.1016/j.cej.2010.01.048.
[68] L. Milne, I. Stewart, D.H. Bremner, Comparison of hydroxyl radical formation in aqueous solutions at different ultrasound frequencies and powers using the salicylic acid dosimeter, Ultrason, Sonochem 20 (3) (2013) 948–989. https://doi.org/10.1016/j.ultsonch.2012.10.020.
[69] C. Yu, J. He, S. Lan, W. Guo, M. Zhu, Enhanced utilization efficiency of peroxymonosulfate via water vortex-driven piezo-activation for removing organic contaminants from water, Environ. Sci. Ecotechnol. 10 (2022), 100165, https://doi.org/10.1016/j.ese.2022.100165.
[70] S. Lan, B. Jing, C. Yu, D. Yan, Z. Li, Z. Ao, M. Zhu, Protrudent iron single-atom accelerated interfacial piezoelectric polarization for self-powered water motion triggered fenton-like reaction, Small 18 (2) (2022), e2105279, https://doi.org/10.1002/smll.202105279.
[71] M.M. Amer, R. Hommelsheim, C. Schumacher, D. Kong, C. Bolm, Electro-mechanochemical approach towards the chloro sulfoximidations of allenes under solvent-free conditions in a ball mill, Faraday Discuss 241 (2023) 79–90, https://doi.org/10.1039/d2fd00075j, 0.